Chemical Science

ROYAL SOCIETY OF CHEMISTRY

EDGE ARTICLE

View Article Online
View Journal | View Issue

Cite this: *Chem. Sci.*, 2020, **11**, 1975

All publication charges for this article have been paid for by the Royal Society of Chemistry

Received 5th November 2019
Accepted 5th January 2020

DOI: 10.1039/c9sc05598c

rsc.li/chemical-science

Isolation of singlet carbene derived 2-phospha-1,3-butadienes and their sequential one-electron oxidation to radical cations and dications†

Mahendra K. Sharma, [a] Sebastian Blomeyer, [a] Timo Glodde, [a] Beate Neumann,[a] Hans-Georg Stammler,[a] Alexander Hinz, [b] Maurice van Gastel[c] and Rajendra S. Ghadwal *[a]

A synthetic strategy for the 2-phospha-1,3-butadiene derivatives [{(IPr)C(Ph)}P(cAAC^{Me})] (**3a**) and [{(IPr)C(Ph)}P(cAAC^{Cy})] (**3b**) (IPr = C{(NDipp)CH}$_2$, Dipp = 2,6-i$Pr_2C_6H_3$; cAAC^{Me} = C{(NDipp)CMe_2CH_2CMe_2}; cAAC^{Cy} = C{(NDipp)CMe_2CH_2C(Cy)}, Cy = cyclohexyl) containing a C=C–P=C framework has been established. Compounds **3a** and **3b** have a remarkably small HOMO–LUMO energy gap (**3a**: 5.09; **3b**: 5.05 eV) with a very high-lying HOMO (−4.95 eV for each). Consequently, **3a** and **3b** readily undergo one-electron oxidation with the mild oxidizing agent $GaCl_3$ to afford radical cations [{(IPr)C(Ph)}P(cAAC^R)]$GaCl_4$ (R = Me **4a**, Cy **4b**) as crystalline solids. The main UV-vis absorption band for **4a** and **4b** is red-shifted with respect to that of **3a** and **3b**, which is associated with the SOMO related transitions. The EPR spectra of compounds **4a** and **4b** each exhibit a doublet due to coupling of the unpaired electron with the ^{31}P nucleus. Further one-electron removal from the radical cations **4a** and **4b** is also feasible with $GaCl_3$, affording the dications [{(IPr)C(Ph)}P(cAAC^R)]$(GaCl_4)_2$ (R = Me **5a**, Cy **5b**) as yellow crystals. The molecular structures of compounds **3–5** have been determined by X-ray diffraction and analyzed by DFT calculations.

Introduction

Organic π-conjugated molecules are currently of great academic and significant technological interest due to their intriguing optoelectronic properties.[1] In this context, π-conjugated systems featuring heavier main-group elements[2] and systems exhibiting a considerable open-shell (radical-type) character[3] are particularly attractive as they display promising optical, electronic, and magnetic properties. Among heavier main-group elements, the choice to incorporate phosphorus into π-conjugated systems has been primarily driven by its semblance to the isoelectronic "CR" (R = H, alkyl or aryl group) unit, which is known as a diagonal relationship.[4] Moreover, while the calculated P=C π-bond strength (43 kcal mol^{-1}) is lower than the C=C π-bond of ethene (65 kcal mol^{-1})[5] the conjugative properties of both P=C and C=C bonds are comparable.[6]

Among stable main-group radicals,[7] various neutral,[8] cationic,[9] as well as anionic[10] phosphorus radicals have been also isolated and structurally characterized, however, phosphorus radicals based on a π-conjugated framework remain scarce. 1,3-Butadiene **I** is the simplest molecule with conjugated π-bonds (Fig. 1) that has also been an important structural motif in phosphorus chemistry.[11] Indeed, unsubstituted as well as alkyl substituted phosphorus containing 1,3-butadiene derivatives were already reported by Appel,[11b] Regitz,[11f] and Denis,[11g] however, these compounds are unlikely to afford stable radical compounds on oxidation or reduction. In 2008, Robinson *et al.* reported a diphosphorus compound **II** containing a weak π-acceptor N-heterocyclic carbene (NHC).[12] Structural and theoretical data suggest that **II** should be better described as a base-stabilized diphosphinidene with $C_{(NHC)}$–P and P–P single bonds. Compound **III**, reported by Bertrand's group in 2010, features a strong π-acceptor cyclic alkyl amino carbene (cAAC^R) and exhibits short C–P bond lengths, thus it may be regarded as a genuine 2,3-diphospha-1,3-butadiene.[13] The same group also reported the 2-phospha-3-azabutadiene **IV** by an elegant choice of imine and cAAC precursors.[9c] Remarkably, these electron-rich species readily undergo one-electron oxidation to afford the corresponding radical cations (**II**)$^{\bullet+}$, (**III**)$^{\bullet+}$, and (**IV**)$^{\bullet+}$.[9b,9c] We recently reported NHC-derived divinyldiphosphenes **V**[14] and isolated the corresponding radicals cations (**V**)$^{\bullet+}$ by one-electron oxidation of **V**.[15] These and other early results[16] prompted us to reason that stable 2-phospha-1,3-butadienes **VI** as well as the corresponding radical cations (**VI**)$^{\bullet+}$ and dications (**VI**)$^{++}$ should be synthetically accessible by a rational choice of substrates and reaction conditions.

[a]*Molecular Inorganic Chemistry and Catalysis, Inorganic and Structural Chemistry, Center for Molecular Materials, Faculty of Chemistry, Universität Bielefeld, Universitätsstrasse 25, Bielefeld, D-33615, Germany. E-mail: rghadwal@uni-bielefeld.de*

[b]*Institute of Inorganic Chemistry, Karlsruhe Institute of Technology (KIT), Engesserstr. 15, D-76131 Karlsruhe, Germany*

[c]*Max-Planck-Institut für Kohlenforschung, Molecular Theory and Spectroscopy, Kaiser-Wilhelm-Platz 1, Mülheim an der Ruhr, D-45470, Germany*

† Electronic supplementary information (ESI) available. CCDC 1949887–1949892 and 1951632. For ESI and crystallographic data in CIF or other electronic format see DOI: 10.1039/c9sc05598c

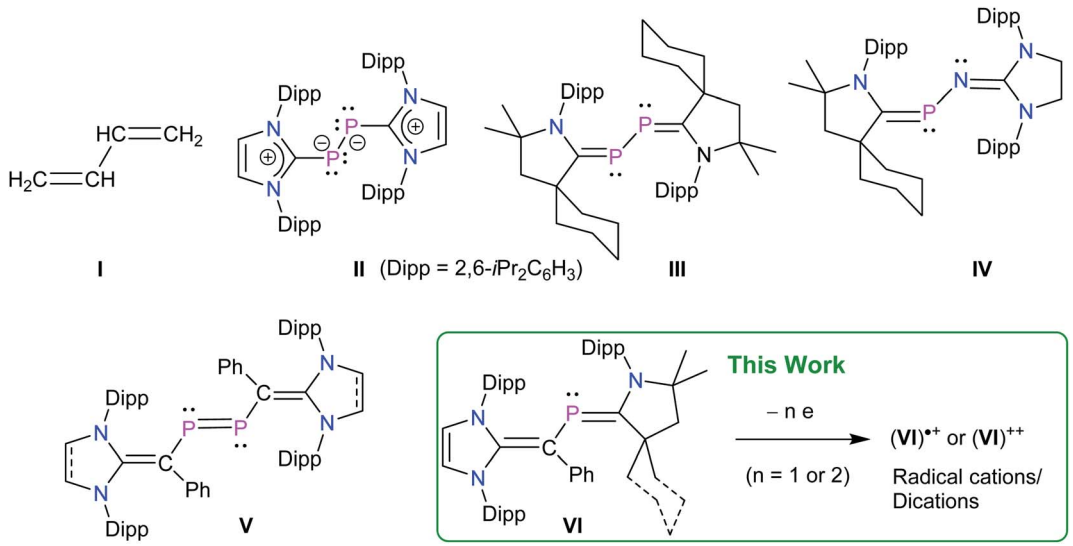

Fig. 1 1,3-Butadiene I. Selected examples of phosphorus containing derivatives II–IV and divinyldiphosphene V with singlet carbene frameworks.

Herein, we report the synthesis of 2-phospha-1,3-butadienes [{(IPr)C(Ph)}P(cAAC^{Me})] (**3a**) and [{(IPr)C(Ph)}P(cAAC^{Cy})] (**3b**) based on singlet carbene frameworks (IPr = C{(NDipp)CH}$_2$, Dipp = 2,6-iPr$_2$C$_6$H$_3$; cAAC^{Me} = C{(NDipp)CMe$_2$CH$_2$CMe$_2$}; cAAC^{Cy} = C{(NDipp)CMe$_2$CH$_2$C(Cy)}, Cy = cyclohexyl) as crystalline solids. Sequential one-electron oxidation of **3a** and **3b** leads to the formation of corresponding radical cations [{(IPr)C(Ph)}P(cAAC^{Me})](GaCl$_4$) (**4a**), [{(IPr)C(Ph)}P(cAAC^{Cy})](GaCl$_4$) (**4b**) and dications [{(IPr)C(Ph)}P(cAAC^{Me})](GaCl$_4$)$_2$ (**5a**), [{(IPr)C(Ph)}P(cAAC^{Cy})] (GaCl$_4$)$_2$ (**5b**) as crystalline solids.

Results and discussion

For the synthesis of desired 2-phospha-1,3-butadienes, N-heterocyclic vinyl (NHV)-substituted dichlorophosphine {(IPr)C(Ph)}PCl$_2$ (**1**)[14] and strong π-acceptor cAAC^R (ref. 17) were chosen as the appropriate precursors (Scheme 1).[18] Treatment of

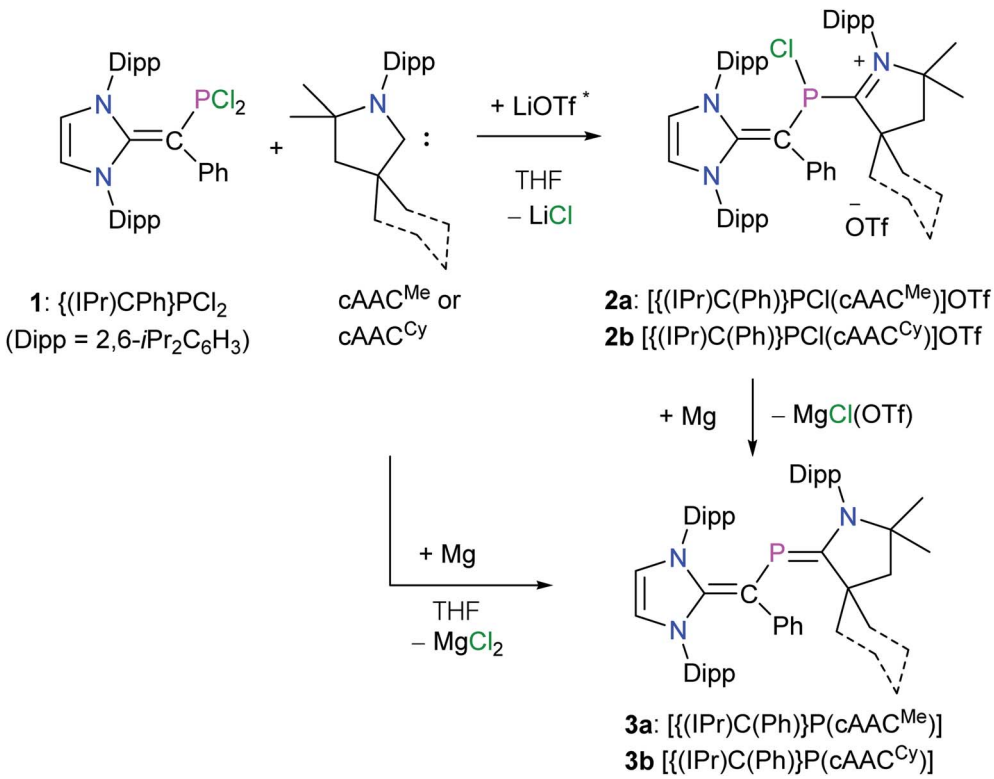

Scheme 1 Synthesis of 2-phospha-1,3-butadiene derivatives **3a** and **3b**. * cAACs were prepared by the deprotonation of their triflate salts with LDA and the side-product LiOTf was not separated.

a colorless THF solution of **1** with one equivalent of $cAAC^{Me}$ or $cAAC^{Cy}$ immediately resulted in the formation of dark blue solutions (Scheme 1). After workup, the ionic compounds [{(IPr)C(Ph)}P(Cl)($cAAC^{R}$)](OTf) (R = Me **2a**, Cy **2b**) were isolated as violet crystalline solids. Compounds **2a** and **2b** are highly air sensitive solids and have been characterized by elemental analysis and NMR spectroscopy. The solid state molecular structure of a typical compound **2a** (Fig. S31†) was determined by X-ray diffraction. Reduction of **2a** and **2b** with magnesium turnings afforded the target compound **3a** and **3b**, respectively, as orange solids. Interestingly, **3a** and **3b** are also accessible in a one-pot reaction of **1** and $cAAC^{R}$ with magnesium. Both **3a** and **3b** are soluble in common organic solvents (*n*-hexane, Et_2O, benzene, toluene, THF) and are stable under an inert gas atmosphere.

The ^{1}H NMR spectra of compounds **2a** and **2b** as well as **3a** and **3b** show expected resonances for the NHV and $cAAC^{R}$ moieties. The $^{13}C\{^1H\}$ NMR spectrum of **2a** and **2b** as well as **3a** and **3b** each is consistent with the ^{1}H NMR resonances and exhibits expected doublets for the phosphorus bound carbon atoms (see the ESI†). The $^{31}P\{^1H\}$ NMR spectrum of **2a** (+100.9 ppm) and **2b** (+102.9 ppm) each shows a singlet, which is high-field shifted with respect to that of the **1** (+167 ppm). This is most likely due to the coordination of electron-rich $cAAC^{R}$ to the phosphorus atoms in **2a** and **2b**. The $^{31}P\{^1H\}$ NMR signal for **3a** (+102.5 ppm) and **3b** (+108.6 ppm), respectively, appears at a higher field compared to that of **IV** (+134.0 ppm),[9c] which is expected because of the electronegativity difference between carbon and nitrogen.

The solid-state molecular structures of **3a** and **3b** (Fig. 2) adopt a *trans*-bent geometry along the C_{NHV}–P bond with the C2–P1 bond length of 1.818(1) and 1.820(1) Å, respectively. The C2–P1 bond length is larger compared to that in **1** (1.728(2) Å)[14] and **2a** (1.751(2) Å), but it is comparable with those of the diphosphenes **V** (1.785 to 1.797 Å).[15] The P1–C3 (**3a**: 1.735(1); **3b** 1.735(1) Å) and C1–C2 (**3a**: 1.386(1); **3b**: 1.384(2) Å) bonds are shorter compared to the same bonds in **2a** (1.860(2) and 1.437(2) Å, respectively). The P1–C3 bond lengths of **3a** and **3b** are nonetheless in line with those of the P=C double bonds in **III** (1.719(7) Å)[13] and **IV** (1.719(2) Å).[9c] The C1=C2, P1=C3, and P1–C2 bond lengths of **3a** and **3b** are in line with those of the literature known neutral 2-phospha-1,3-butadiene (Me_3SiO)*t*BuC=P–C($SiMe_3$)=C($OSiiPr_3$)*t*Bu (C=C: 1.356(4), P=C: 1.702(3), P–C: 1.846(3) Å).[19]

To shed light on the electronic structure of **3a** and **3b**, we performed DFT calculations at the M06-2X/def2-TZVPP//def2-SVP level of theory. The HOMO of **3a** and **3b** is a π-type orbital mainly located at the C_{cAAC}=P and C_{IPr}=C_{Ph} bonds (Fig. 3). Remarkably, the HOMO energy of **3a** and **3b** (−4.95 eV) is quite high and comparable with those of related divinyldiphosphenes **V** (−4.71 to −5.25 eV),[15] indicating the possibility of facile oxidation.

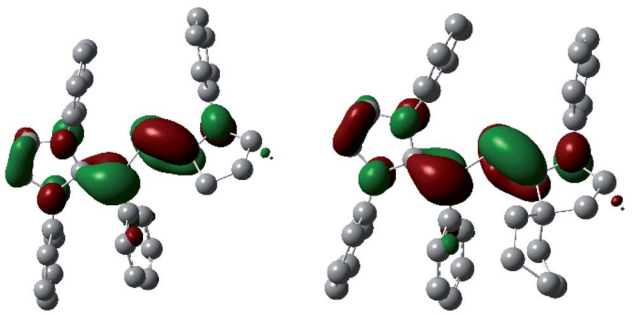

Fig. 3 HOMOs (highest occupied molecular orbitals, isovalue 0.04) of **3a** and **3b** calculated at M06-2X/def2-TZVPP//def2-SVP level of theory. Hydrogen atoms, methyl as well as iso-propyl groups were omitted for clarity.

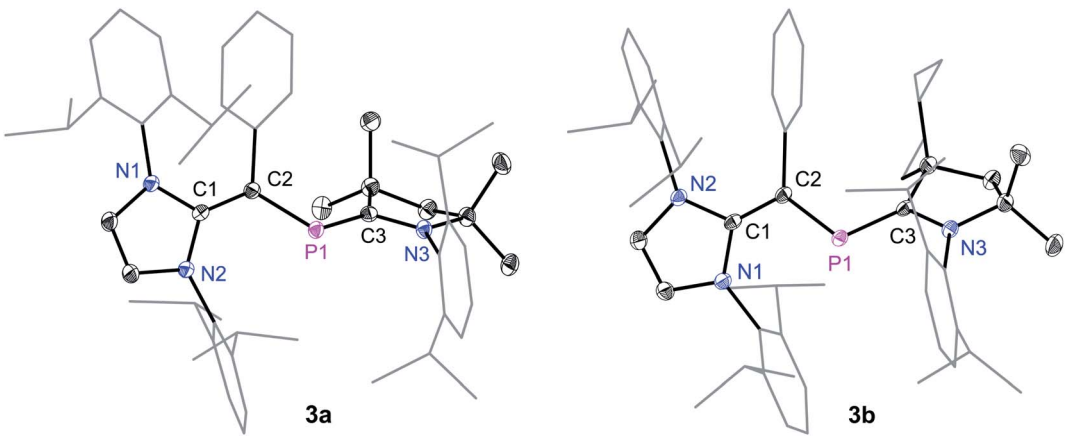

Fig. 2 Solid-state molecular structures of 2-phospha-1,3-butadienes **3a** and **3b**. Hydrogen atoms have been omitted for clarity. Selected bond lengths and bond angles are given in Table 1.

These preliminarily theoretical findings encouraged us to analyze the redox properties of **3a** and **3b** by electrochemical studies to gain an initial insight into the viability and stability of derived radicals. The cyclic voltammograms (CVs) of **3a** (Fig. S19†) and **3b** (Fig. S20†) show two main redox events in the −2.0 to 1.5 V region. The first reversible wave at $E_{1/2} = -1.06$ V for **3a** and −1.08 V for **3b** may be assigned to the corresponding radical cation, whereas the second quasi-reversible wave at $E_{1/2} = -0.28$ V for **3a** and −0.24 V for **3b** may correspond to the dicationic species. Indeed, treatment of an orange toluene solution of **3a** or **3b** with $GaCl_3$ immediately led to the precipitation of a violet solid. After workup, the radical cation salts [{(IPr)C(Ph)}P(cAAC^{Me})][$GaCl_4$] (**4a**) and [{(IPr)C(Ph)}P(cAAC^{Cy})][$GaCl_4$] (**4b**) were isolated as violet crystals (Scheme 2). $GaCl_3$ acts as oxidizing agent and two molecules of $GaCl_3$ are required for one-electron oxidation.[15] Consistent with the CVs (Fig. S19 and S20†), the dication salts [{(IPr)C(Ph)}P(cAAC^{Me})][$GaCl_4$]$_2$ (**5a**) and [{(IPr)C(Ph)}P(cAAC^{Cy})][$GaCl_4$]$_2$ (**5b**) are selectively accessible on one-electron oxidation of **4a** and **4b** with $GaCl_3$ (Scheme 2). Alternatively, **5a** and **5b** can also be prepared directly from **3a** and **3b** with four equivalent of $GaCl_3$, respectively (Scheme 2). Compounds **4a**, **4b** and **5a**, **5b** are stable both in solutions as well as in the solid-state under an inert gas atmosphere, but decompose rapidly when exposed to air. The radicals **4a** and **4b** are NMR silent, while dicationic salts **5a** and **5b** are diamagnetic and exhibit well resolved ^{1}H and ^{13}C{^{1}H} NMR signals for the NHV and cAAC^R units. The ^{31}P{^{1}H} NMR signal for the dication salts **5a** (+244 ppm) and **5b** (+236 ppm) is downfield-shifted with respect to that of the 2-phospha-1,3-butadienes **3a** (+102 ppm) and **3b** (+108 ppm) but it is in the range expected for phosphaalkenes (200–300 ppm).[20]

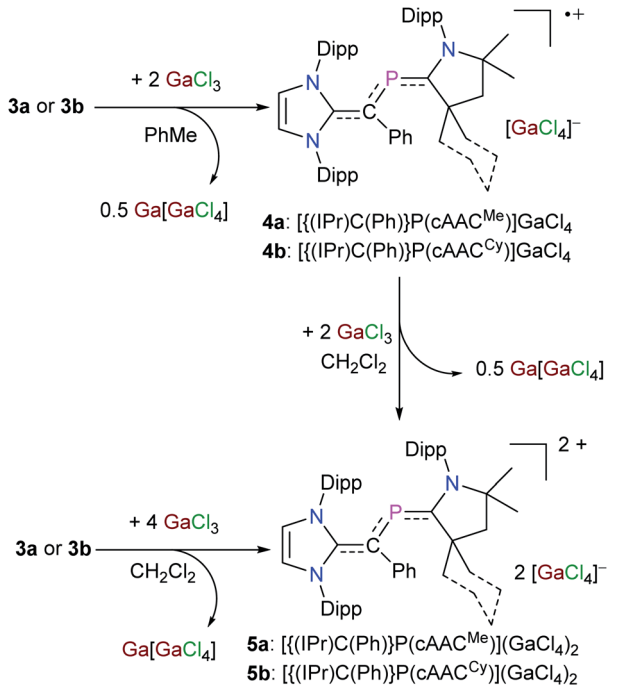

Scheme 2 Sequential one-electron oxidation of 2-phospha-1,3-butadienes **3a** and **3b** with $GaCl_3$ to the corresponding radical cations **4a** and **4b** and dications **5a** and **5b**.

Suitable single crystals for X-ray diffraction were obtained by a slow diffusion of *n*-hexane into a saturated THF or CH_2Cl_2 solution of each of radical cations **4a** and **4b** and dicationic salts **5a** and **5b**. The solid-state molecular structure of **4a** and **4b** (Fig. 4) as well as **5a** and **5b** (Fig. 5) each adopts a *trans*-bent geometry along the P–C_{NHV} bond and reveals an interesting bond length alteration trend with

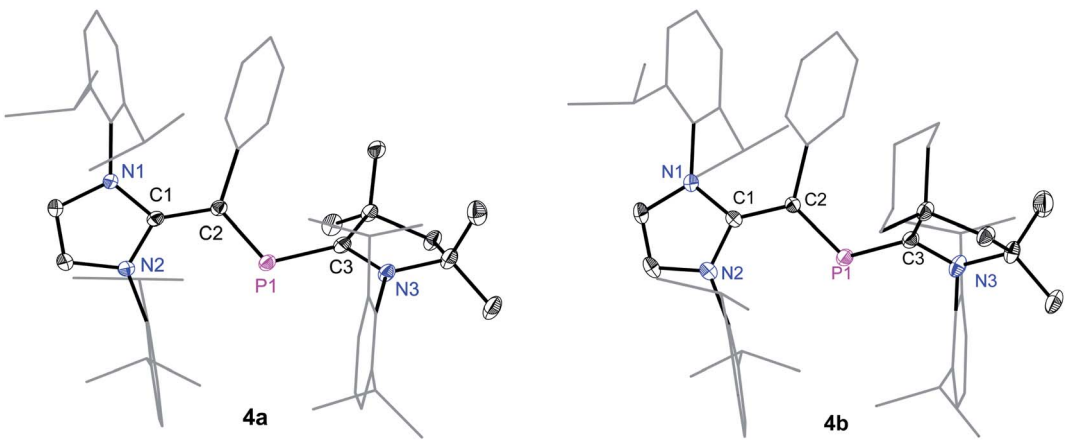

Fig. 4 Solid-state molecular structures of radical cation **4a** and **4b**. Hydrogen atoms, solvent molecules in **4b**, and the counter anions $GaCl_4$ have been omitted for clarity. Selected bond lengths and bond angles are given in Table 1.

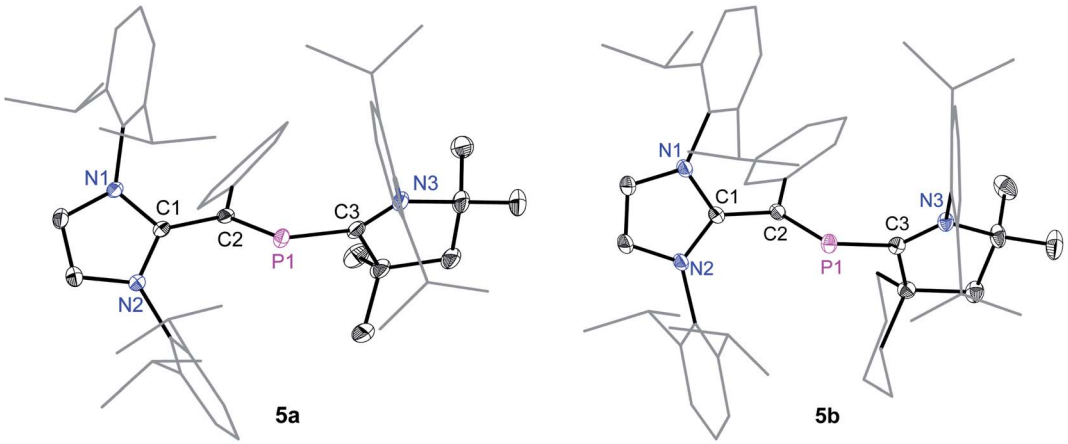

Fig. 5 Solid-state molecular structures of **5a** and **5b**. Hydrogen atoms, solvent molecules in **5b**, and the counter anions $GaCl_4$ have been omitted for clarity. Selected bond lengths and bond angles are given in Table 1.

respect to the precursors **3a** and **3b** (Table 1). The C2–P1 bond length of **4a** (1.758(2) Å) and **4b** (1.761(2) Å) is smaller compared to that of the respective 2-phospha-1,3-butadienes **3a** (1.818(1) Å) and **3b** (1.820(1) Å) but longer with respect to that of the dications **5a** (1.692(3) Å) and **5b** (1.692(2) Å) Å. The P1–C3 bond, however, steadily stretches on going from neutral to radical cations and to dications: **3a**: 1.735(1), **3b**: 1.735(1); **4a**: 1.785(2), **4b**: 1.790(2); **5a**: 1.865(2), **5b**: 1.853(2) Å. A similar trend in the C1–C2 bond length stretching can also be seen in **3a**: 1.386(1), **3b**: 1.384(2); **4a**: 1.432(2), **4b**: 1.433(2); and **5a**: 1.479(3), **5b**: 1.478(2) Å. In conclusion, the formally C1=C2 and P1=C3 double bonds in **3a** and **3b** become comparable to C_{sp^2}–C_{sp^2} (*ca.* 1.47 Å) and P–C_{sp^2} (1.85 Å) single bond lengths[21] in **5a** and **5b**, whereas the C2–P1 single bond in **3a** and **3b** adopts double bond lengths (1.60–1.70 Å) in **5a** and **5b** as expected for phosphaalkenes.[22]

Table 1 Selected bond lengths (Å) and angles (°) of 2-phospha-1,3-butadienes (**3a** and **3b**), radical cations (**4a** and **4b**) and dication salts (**5a** and **5b**)

	3a	3b	4a	4b	5a	5b
C1–C2	1.386(1)	1.384(2)	1.432(2)	1.433(2)	1.479(3)	1.478(2)
C2–P1	1.818(1)	1.820(1)	1.758(2)	1.761(2)	1.692(2)	1.692(2)
P1–C3	1.735(1)	1.735(1)	1.785(2)	1.790(2)	1.865(2)	1.853(2)
C1–N1	1.401(1)	1.403(1)	1.375(2)	1.375(2)	1.351(3)	1.344(2)
C1–N2	1.408(1)	1.412(1)	1.382(2)	1.385(2)	1.355(3)	1.356(2)
C3–N3	1.387(1)	1.388(1)	1.349(2)	1.349(2)	1.295(3)	1.295(3)
C1–C2–P1	117.7(1)	118.0(1)	117.3(1)	117.4(1)	114.9(1)	115.3(1)
C2–P1–C3	109.7(1)	110.9(1)	108.8(1)	110.3(1)	106.1(1)	105.2(1)
P1–C3–N3	117.6(1)	116.4(1)	116.0(1)	115.1(1)	118.1(2)	121.5(1)
N1–C1–N2	103.0(1)	103.3(1)	104.8(1)	104.9(1)	107.2(2)	107.3(2)

DFT calculated geometries of **3–5** are found to be fully in agreement with their solid-state molecular structures determined by X-ray diffraction (Table S5†). An increasing value of the WBIs (Wiberg Bond Indices) for the C_{NHV}–P bond of **3a** (0.95), **3b** (0.95), **4a** (1.22), **4b** (1.22), **5a** (1.63), and **5b** (1.63) is consistent with the experimental C2–P1 bond lengths (Table 1). Similarly, the WBIs for the P–C_{cAAC} (**3a**: 1.57, **3b**: 1.56; **4a**: 1.19, **4b**: 1.18; **5a**: 0.92, **5b**: 0.91) as well as C–C_{Ph} (**3a**: 1.49, **3b**: 1.49; **4a**: 1.20, **4b**: 1.20; **5a**: 1.06, **5b**: 1.06) bonds also exhibit the expected trend. The NPA (Natural Population Analysis) atomic partial charges (Table S5†) calculated using the NBO (Natural Bond Orbital) method indicate that the phosphorous atom in **3a** (0.49*e*), **3b** (0.49*e*), **4a** (0.65*e*), **4b** (0.65*e*), **5a** (0.85*e*), and **5b** (0.85*e*) carries a positive charge. The former IPr carbene carbon atom (C1) also bears a positive charge (**3a** 0.45*e*, **3b** 0.44*e*, **4a** 0.47*e*, **4b** 0.47*e*, **5a** 0.43*e* and **5b** 0.43*e*), which is larger compared to that of the cAAC carbene carbon atom C3 (**3a** −0.08*e*, **3b** −0.08*e*, **4a** 0.04*e*, **4b** 0.04*e*, **5a** 0.23*e* and **5b** 0.24*e*). This is most likely because of the greater π-acceptor property of cAACs compared to the IPr.

The SOMO (singly occupied molecular orbital) of **4a** and **4b** (Fig. 6) is the π-orbitals of the C_{IPr}=C_{vinyl} and P=C_{cAAC} bonds with a small contribution from the nitrogen atoms of the pyrrolidine and imidazole ring, whereas the LUMO (lowest unoccupied molecular orbital) is the π*-orbitals of the P atom along with the π*-orbitals of C_{IPr}=C_{vinyl} and C_{cAAC}–N bonds of NHV and cAAC, respectively. The localized Mulliken atomic spin density (Fig. 7) and the plot of the SOMO (Fig. 6) for **4a** and **4b** reveal that the unpaired electron is mainly delocalized over the CPCN moiety with an almost equal spin density distribution on the phosphorus (**4a**: 17%, **4b**: 18%), carbene C_{cAAC} (**4a**: 19%, **4b**: 20%), and vinylic C_{Ph} (**4a**: 26%, **4b**: 25%) atoms. The spin-density at the imidazole-ring nitrogen atoms (6% at each of N) of **4a** and **4b** is rather small compared to that at the pyrrolidine nitrogen atom (17%).

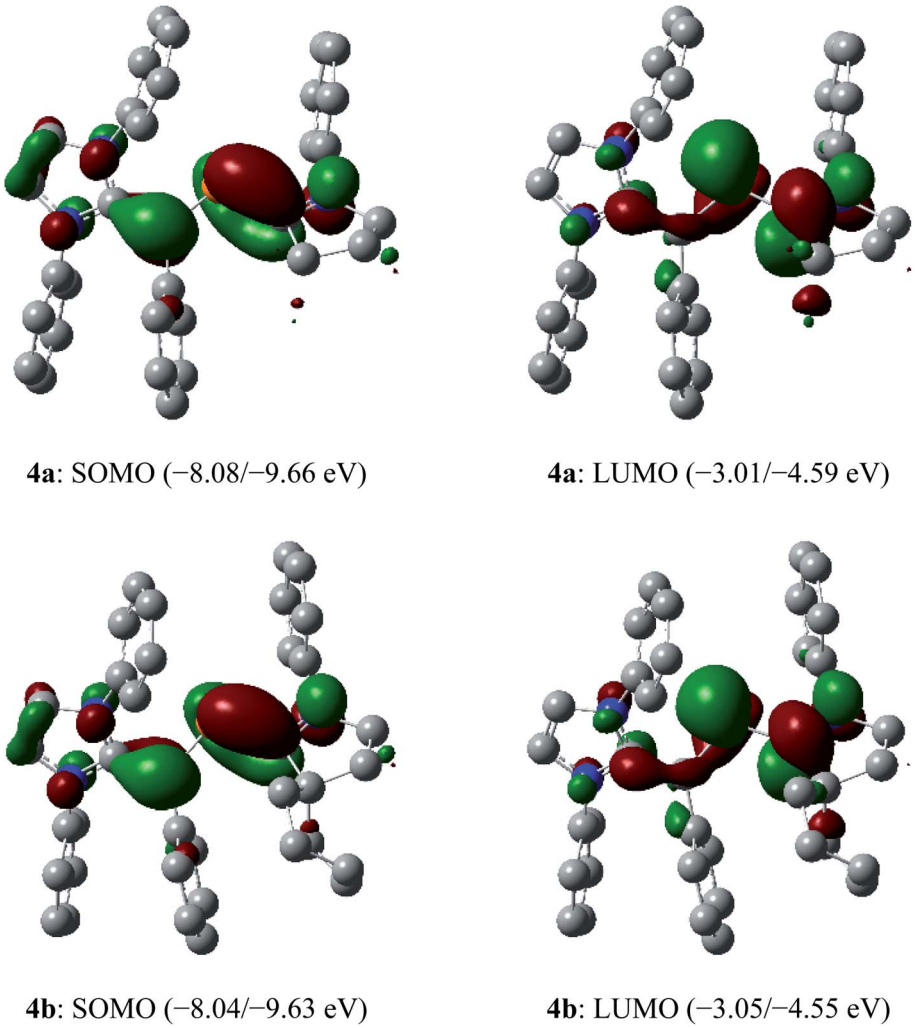

Fig. 6 Selected molecular orbitals (isovalue 0.04) of the radical cations **4a** and **4b** (α/β spin orbital energy) calculated at the M06-2X/def2-TZVPP//def2-SVP level of theory. Hydrogen atoms, methyl groups as well as iso-propyl groups were omitted for clarity.

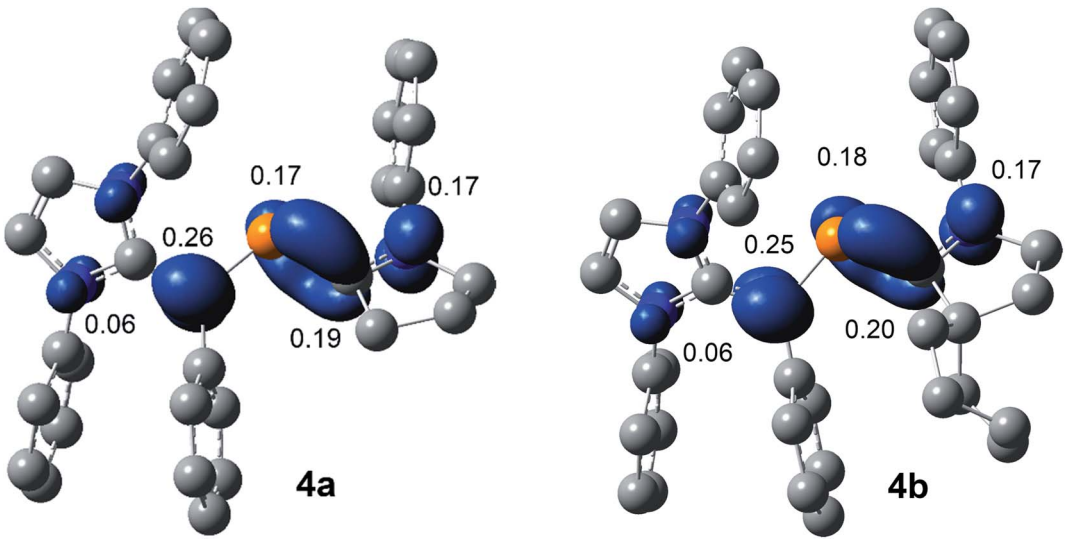

Fig. 7 Calculated Mulliken spin densities (isovalue 0.004 a.u.) of radical cations **4a** and **4b** at M06-2X/def2-TZVPP//def2-SVP level of theory.

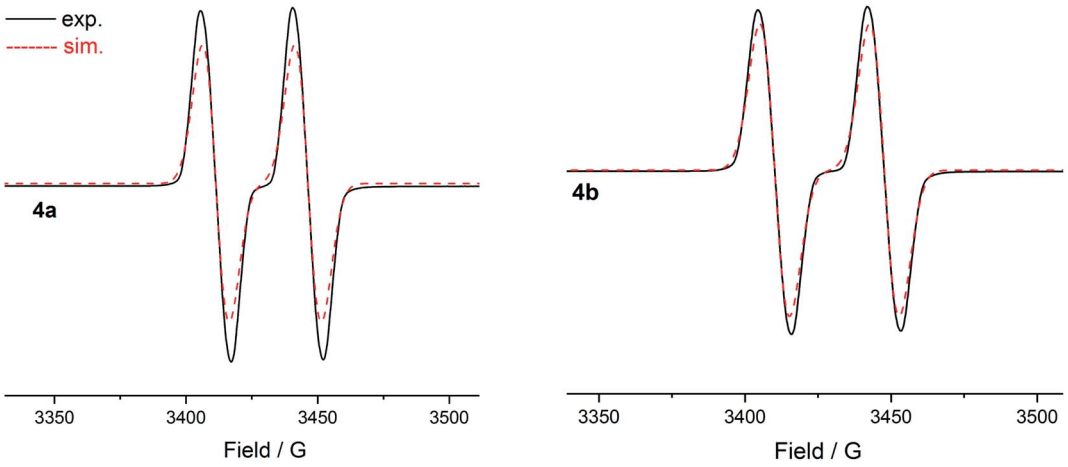

Fig. 8 X-band EPR spectra of radical cations **4a** and **4b** in THF at 298 K.

The room temperature X-band EPR spectra of **4a** (g = 2.0064) and **4b** (g = 2.0064) in THF exhibit a doublet (Fig. 8) owing to the coupling of the unpaired electron with the phosphorous nucleus ($A_{iso}(^{31}P)$ = 35 G **4a**; 38 G **4b**). The magnitude of the hyperfine coupling constant (hfc) of **4a** and **4b** is comparable to those observed for radical cations $(\mathbf{II})^{\bullet+}$ ($A_{iso}(^{31}P)$ = 44 G)[9b] $(\mathbf{III})^{\bullet+}$ ($A_{iso}(^{31}P)$ = 42 G),[9b] and $(\mathbf{IV})^{\bullet+}$ ($A_{iso}(^{31}P)$ = 44 G),[9c] but that is larger than those of $(\mathbf{V})^{\bullet+}$ ($A_{iso}(^{31}P)$ = 12–20 G) featuring a longer π-conjugated system (Fig. 1).[15] This is, however, considerably smaller than that of the phosphinyl radical cation $[(cAAC^{Cy})P(R)]^{\bullet+}$ ($A_{iso}(^{31}P)$ = 99 G) (R = 2,2,6,6-tetramethylpiperidino)[9a] as well as those observed for phosphinyl radicals $R_2P^{\bullet}$ ($A_{iso}(^{31}P)$ = 92–96 G) (R = $HC(SiMe_3)_2$ or $N(SiMe_3)_2$),[8a,23] for which, particularly for the latter, the unpaired electron resides predominantly in a 3p(P) valence orbital. The value of coupling constants is in good agreement with the computed values (Table S12†). These hfcs corroborate with the delocalization of the spin-density along the CPCN moiety of **4a** and **4b** (Fig. 7). The measured EPR spectra of **4a** and **4b** were simulated by employing the g values, the hyperfine coupling for the phosphorus atom, and two linewidth parameters (Table S13†). The EPR spectra of **4a** (Fig. S29†) and **4b** (Fig. S30†) measured in a frozen THF solution at 80 K show an anisotropic pattern. The g-factors (**4a**: $g_{\parallel}$ = 2.0062, $g_{\perp}$ = 2.0082; **4b**: $g_{\parallel}$ = 2.0069, $g_{\perp}$ = 2.0079) and hfc tensors (**4a**: $A_z(^{31}P)$ = 149 MHz, $A_x(^{31}P)$ = −83 MHz, $A_y(^{31}P)$ = 39 MHz; **4b**: $A_z(^{31}P)$ = 179 MHz, $A_x(^{31}P)$ = −71 MHz, $A_y(^{31}P)$ = 49 MHz) were determined. The analysis of hfc tensors reveals the major contribution of phosphorus 3p (**4a**: 11.8%; **4b**: 12.8%) orbital to the SOMO, whereas the contribution of the 3s (**4a**: 0.45%; **4b**: 0.46%) orbital is small.

The UV-vis spectra of both 2-phospha-1,3-butadienes **3a** (277, 331, 427 nm) and **3b** (271, 322, 430 nm) exhibit three main absorptions (Fig. 9) which, based on TD-DFT calculations at TD-PCM(thf)/M06-2X/def2-SVP level of theory, comprise dominant contributions of the H−1 → L, H → L+2, and H → L transitions, respectively (Fig. S32 and S33, Tables S6 and S7†). The UV-vis spectra of the radical cations **4a** and **4b**, respectively show a broad absorption at 563 and 571 nm along with a shoulder at *ca.* 700 nm (Fig. 9) that corresponds to the SOMO-related transitions S → L and S−1 → S (Tables S8 and S9†).

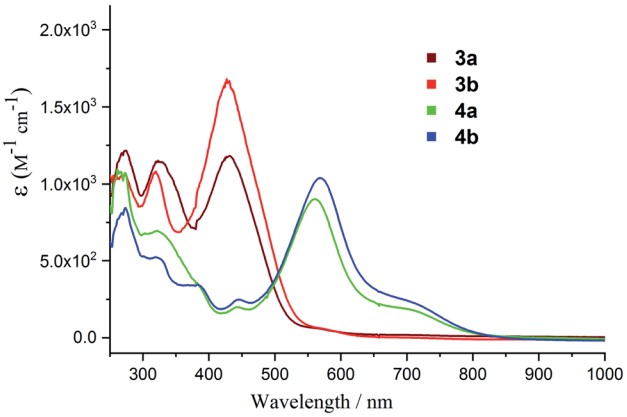

Fig. 9 UV-vis spectra of **3a** and **3b** and their radical cations **4a** and **4b** in THF.

In the dications **5a** and **5b**, the HOMO-2 is a π-type orbital with contributions from the aryl groups and C_{vinyl}–P bond (Fig. 10). The LUMO of **5a** and **5b** is the π-orbital of the C_{IPr}=C_{vinyl} and P=C_{cAAC} bonds with a small contribution from the nitrogen atoms of pyrrolidine and imidazole rings. Upon removal of one and two electrons from the π-type orbital of **3a** and **3b**, the HOMO of **3a** and **3b** (Fig. 3) becomes SOMO in the radical cations **4a** and **4b** (Fig. 6) and LUMO in the dications **5a** and **5b** (Fig. 10).

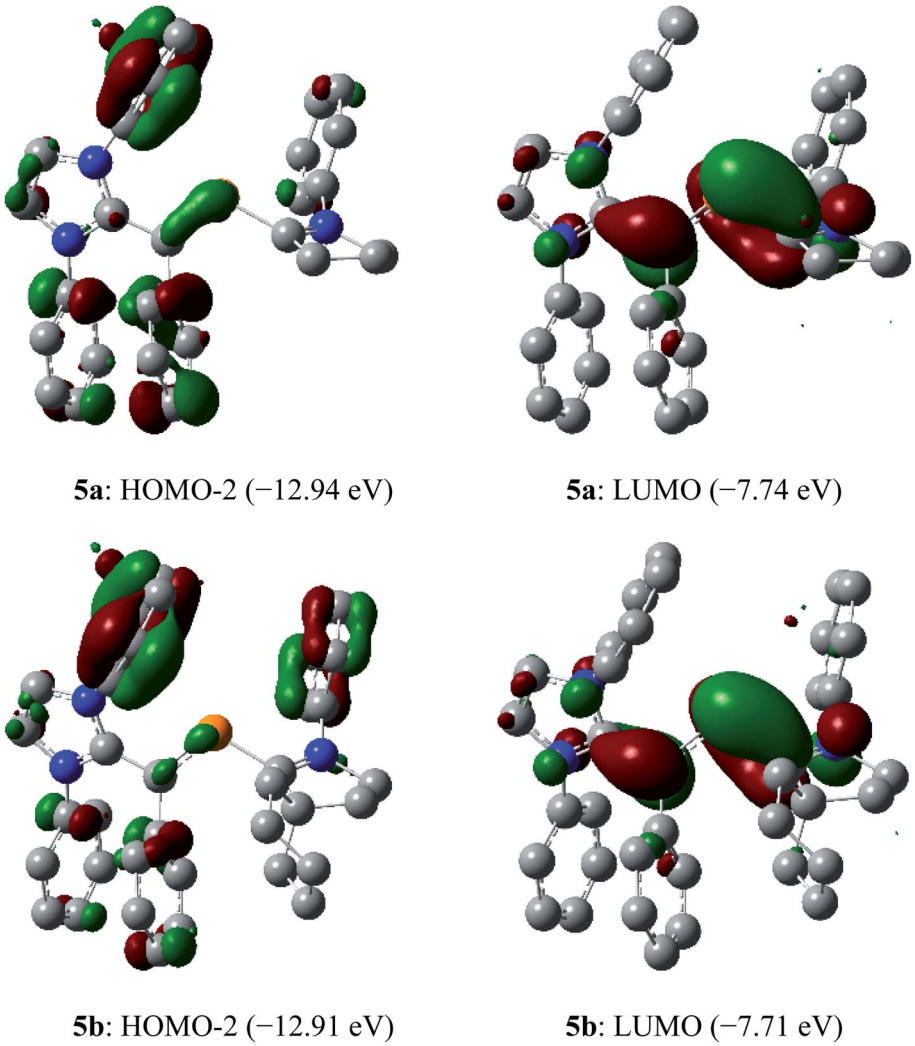

Fig. 10 Selected molecular orbitals (isovalue 0.04) of the dications **5a** and **5b** calculated at M06-2X/def2-TZVPP//def2-SVP level of theory. Hydrogen atoms, methyl groups as well as iso-propyl groups were omitted for clarity.

Conclusions

In conclusion, we have isolated the crystalline 2-phospha-1,3-butadiene derivatives **3a** and **3b** by a rational choice of combining a weak π-acceptor (IPr) and a strong π-acceptor ($cAAC^R$) singlet carbene scaffolds. Sequential one-electron oxidation of **3a** and **3b** affords the radical cations **4a** and **4b** and the dications **5a** and **5b**. The isolation of **4a**, **4b** and **5a**, **5b** as crystalline solids is consistent with the redox properties of **3a** and **3b** analyzed by electrochemical studies. Molecular structures of all compounds in the solid-state were established by single crystal X-ray diffraction. Computational and EPR spectroscopic data indicate that the unpaired electron in **4a** and **4b** is delocalized over the CPCN π-conjugated framework. The study emphasizes the advantage of merging singlet carbenes with dissimilar donor–acceptor properties in accessing stable open-shell π-conjugated systems. As a variety of stable singlet carbenes with adaptable properties are readily accessible, it is very likely that many π-conjugated systems with other heavier main-group elements, which are hitherto believed to be synthetically challenging targets, may be isolated.

Conflicts of interest

There are no conflicts to declare.

Acknowledgements

We are grateful to the Deutsche Forschungsgemeinschaft (DFG) for financial support and thank Professor Norbert W. Mitzel for his constant support. The authors gratefully acknowledge the support by computing time provided by the Paderborn Center for Parallel Computing (PC2).

References

1 (*a*) C. Wang, H. Dong, W. Hu, Y. Liu and D. Zhu, *Chem. Rev.*, 2012, **112**, 2208–2267; (*b*) W. Wu, Y. Liu and D. Zhu, *Chem.*

Soc. Rev., 2010, **39**, 1489–1502; (*c*) Y. Wang, L. Sun, C. Wang, F. Yang, X. Ren, X. Zhang, H. Dong and W. Hu, *Chem. Soc. Rev.*, 2019, **48**, 1492–1530; (*d*) J. Yang, D. Yan and T. S. Jones, *Chem. Rev.*, 2015, **115**, 5570–5603; (*e*) C. Lee, S. Lee, G.-U. Kim, W. Lee and B. J. Kim, *Chem. Rev.*, 2019, **119**, 8028–8086.

2 (*a*) F. Vidal and F. Jäkle, *Angew. Chem., Int. Ed.*, 2019, **58**, 5846–5870; (*b*) F. Pop, N. Zigon and N. Avarvari, *Chem. Rev.*, 2019, **119**, 8435–8478; (*c*) M. Stolar and T. Baumgartner, *Chem. Commun.*, 2018, **54**, 3311–3322; (*d*) M. Hirai, N. Tanaka, M. Sakai and S. Yamaguchi, *Chem. Rev.*, 2019, **119**, 8291–8331; (*e*) K. Dhbaibi, L. Favereau and J. Crassous, *Chem. Rev.*, 2019, **119**, 8846–8953; (*f*) T. Baumgartner and R. Réau, *Chem. Rev.*, 2006, **106**, 4681–4727; (*g*) S. M. Parke, M. P. Boone and E. Rivard, *Chem. Commun.*, 2016, **52**, 9485–9505; (*h*) A. M. Priegert, B. W. Rawe, S. C. Serin and D. P. Gates, *Chem. Soc. Rev.*, 2016, **45**, 922–953.

3 (*a*) Z. Zeng, X. Shi, C. Chi, J. T. Lopez Navarrete, J. Casado and J. Wu, *Chem. Soc. Rev.*, 2015, **44**, 6578–6596; (*b*) T. Y. Gopalakrishna, W. Zeng, X. Lu and J. Wu, *Chem. Commun.*, 2018, **54**, 2186–2199; (*c*) M. Nakano, K. Fukuda, S. Ito, H. Matsui, T. Nagami, S. Takamuku, Y. Kitagawa and B. Champagne, *J. Phys. Chem. A*, 2017, **121**, 861–873; (*d*) M. Nakano, *Chem. Rec.*, 2017, **17**, 27–62; (*e*) Y. Yang, E. R. Davidson and W. Yang, *Proc. Natl. Acad. Sci. U. S. A.*, 2016, **113**, E5098–E5107; (*f*) Y. Su, X. Wang, X. Zheng, Z. Zhang, Y. Song, Y. Sui, Y. Li and X. Wang, *Angew. Chem., Int. Ed.*, 2014, **53**, 2857–2861; (*g*) J. Casado, *Top. Curr. Chem.*, 2017, **375**, 73.

4 (*a*) M. C. Simpson and J. D. Protasiewicz, *Pure Appl. Chem.*, 2013, **85**, 801–815; (*b*) D. A. Pantazis, J. E. McGrady, J. M. Lynam, C. A. Russell and M. Green, *Dalton Trans.*, 2004, 2080–2086; (*c*) K. B. Dillon, F. Mathey and J. F. Nixon, *Phosphorus: The Carbon Copy*, John Wiley & Sons, New York 1998.

5 (*a*) M. W. Schmidt, P. N. Truong and M. S. Gordon, *J. Am. Chem. Soc.*, 1987, **109**, 5217–5227; (*b*) P. v. R. Schleyer and D. Kost, *J. Am. Chem. Soc.*, 1988, **110**, 2105–2109.

6 (*a*) R. C. Fischer and P. P. Power, *Chem. Rev.*, 2010, **110**, 3877–3923; (*b*) L. Nyulaszi, T. Veszpremi and J. Reffy, *J. Phys. Chem.*, 1993, **97**, 4011–4015; (*c*) R. Szűcs, P.-A. Bouit, L. Nyulászi and M. Hissler, *ChemPhysChem*, 2017, **18**, 2618–2630; (*d*) L. Nyulászi, *Chem. Rev.*, 2001, **101**, 1229–1246.

7 (*a*) R. G. Hicks, *Stable Radicals: Fundamentals and Applied Aspects of Odd-Electron Compounds*, John Wiley & Sons Ltd, Chichester, 2010; (*b*) S. Kundu, S. Sinhababu, V. Chandrasekhar and H. W. Roesky, *Chem. Sci.*, 2019, **10**, 4727–4741; (*c*) G. W. Tan and X. P. Wang, *Chin. J. Chem.*, 2018, **36**, 573–586; (*d*) Y. Kim and E. Lee, *Chem.–Eur. J.*, 2018, **24**, 19110–19121; (*e*) Y. Su and R. Kinjo, *Coord. Chem. Rev.*, 2017, **352**, 346–378; (*f*) M. Soleilhavoup and G. Bertrand, *Acc. Chem. Res.*, 2015, **48**, 256–266; (*g*) C. D. Martin, M. Soleilhavoup and G. Bertrand, *Chem. Sci.*, 2013, **4**, 3020–3030; (*h*) T. Chivers and J. Konu, in *Comprehensive Inorganic Chemistry II: From Elements to Applications*, ed. J. Reedijk and K. Poeppelmeier, Elsevier, Amsterdam, 2013, vol. I, pp. 349–373; (*i*) J. Konu and T. Chivers, in *Stable Radicals: Fundamental and Applied Aspects of Odd-Electron Compounds*, ed. R. G. Hicks, John Wiley & Sons, Ltd, 2010, pp. 381–406; (*j*) F. Breher, *Coord. Chem. Rev.*, 2007, **251**, 1007–1043; (*k*) P. P. Power, *Chem. Rev.*, 2003, **103**, 789–809; (*l*) H. Grützmacher and F. Breher, *Angew. Chem., Int. Ed.*, 2002, **41**, 4006–4011; (*m*) K. C. Mondal, S. Roy and H. W. Roesky, *Chem. Soc. Rev.*, 2016, **45**, 1080–1111.

8 (*a*) S. L. Hinchley, C. A. Morrison, D. W. H. Rankin, C. L. B. Macdonald, R. J. Wiacek, A. H. Cowley, M. F. Lappert, G. Gundersen, J. A. C. Clyburne and P. P. Power, *Chem. Commun.*, 2000, 2045–2046; (*b*) A. Armstrong, T. Chivers, M. Parvez and R. T. Boeré, *Angew. Chem., Int. Ed.*, 2004, **43**, 502–505; (*c*) S. Ito, M. Kikuchi, M. Yoshifuji, A. J. Arduengo III, T. A. Konovalova and L. D. Kispert, *Angew. Chem., Int. Ed.*, 2006, **45**, 4341–4345; (*d*) P. Agarwal, N. A. Piro, K. Meyer, P. Müller and C. C. Cummins, *Angew. Chem., Int. Ed.*, 2007, **46**, 3111–3114; (*e*) O. Back, B. Donnadieu, M. von Hopffgarten, S. Klein, R. Tonner, G. Frenking and G. Bertrand, *Chem. Sci.*, 2011, **2**, 858–861; (*f*) T. Beweries, R. Kuzora, U. Rosenthal, A. Schulz and A. Villinger, *Angew. Chem., Int. Ed.*, 2011, **50**, 8974–8978; (*g*) A. Hinz, A. Schulz and A. Villinger, *Angew. Chem., Int. Ed.*, 2015, **54**, 668–672; (*h*) L. Gu, Y. Zheng, E. Haldón, R. Goddard, E. Bill, W. Thiel and M. Alcarazo, *Angew. Chem., Int. Ed.*, 2017, **56**, 8790–8794; (*i*) X. Chen, A. Hinz, J. R. Harmer and Z. Li, *Dalton Trans.*, 2019, **48**, 2549–2553; (*j*) Z. Li, Y. Hou, Y. Li, A. Hinz, J. R. Harmer, C.-Y. Su, G. Bertrand and H. Grützmacher, *Angew. Chem., Int. Ed.*, 2018, **57**, 198–202; (*k*) A. M. Tondreau, Z. Benko, J. R. Harmer and H. Grützmacher, *Chem. Sci.*, 2014, **5**, 1545–1554.

9 (*a*) O. Back, M. A. Celik, G. Frenking, M. Melaimi, B. Donnadieu and G. Bertrand, *J. Am. Chem. Soc.*, 2010, **132**, 10262–10263; (*b*) O. Back, B. Donnadieu, P. Parameswaran, G. Frenking and G. Bertrand, *Nat. Chem.*, 2010, **2**, 369–373; (*c*) R. Kinjo, B. Donnadieu and G. Bertrand, *Angew. Chem., Int. Ed.*, 2010, **49**, 5930–5933; (*d*) G. Ménard, J. A. Hatnean, H. J. Cowley, A. J. Lough, J. M. Rawson and D. W. Stephan, *J. Am. Chem. Soc.*, 2013, **135**, 6446–6449; (*e*) X. Pan, Y. Su, X. Chen, Y. Zhao, Y. Li, J. Zuo and X. Wang, *J. Am. Chem. Soc.*, 2013, **135**, 5561; (*f*) X. Pan, X. Chen, T. Li, Y. Li and X. Wang, *J. Am. Chem. Soc.*, 2013, **135**, 3414–3417; (*g*) Y. Su, X. Zheng, X. Wang, X. Zhang, Y. Sui and X. Wang, *J. Am. Chem. Soc.*, 2014, **136**, 6251–6254; (*h*) A. Brückner, A. Hinz, J. B. Priebe, A. Schulz and A. Villinger, *Angew. Chem., Int. Ed.*, 2015, **54**, 7426–7430; (*i*) X. Pan, X. Wang, Z. Zhang and X. Wang, *Dalton Trans.*, 2015, **44**, 15099–15102.

10 (*a*) T. Cantat, F. Biaso, A. Momin, L. Ricard, M. Geoffroy, N. Mézailles and P. Le Floch, *Chem. Commun.*, 2008, 874–876; (*b*) C. Pi, Y. Wang, W. Zheng, L. Wan, H. Wu, L. Weng, L. Wu, Q. Li and P. v. R. Schleyer, *Angew. Chem., Int. Ed.*, 2010, **49**, 1842–1845; (*c*) X. Pan, X. Wang, Y. Zhao, Y. Sui and X. Wang, *J. Am. Chem. Soc.*, 2014, **136**, 9834–9837; (*d*) G. Tan, S. Li, S. Chen, Y. Sui, Y. Zhao and

X. Wang, *J. Am. Chem. Soc.*, 2016, **138**, 6735–6738; (*e*) S.-s. Asami, S. Ishida, T. Iwamoto, K. Suzuki and M. Yamashita, *Angew. Chem., Int. Ed.*, 2017, **56**, 1658–1662; (*f*) M. K. Mondal, L. Zhang, Z. Feng, S. Tang, R. Feng, Y. Zhao, G. Tan, H. Ruan and X. Wang, *Angew. Chem., Int. Ed.*, 2019, **58**, 15829–15833.

11 (*a*) R. Appel, U. Kündgen and F. Knoch, *Chem. Ber.*, 1985, **118**, 1352–1370; (*b*) R. Appel, F. Knoch and H. Kunze, *Chem. Ber.*, 1984, **117**, 3151–3159; (*c*) R. Appel, V. Barth and F. Knoch, *Chem. Ber.*, 1983, **116**, 938–950; (*d*) B. Breit, H. Memmesheimer, R. Boese and M. Regitz, *Chem. Ber.*, 1992, **125**, 729–732; (*e*) M. Seidl, M. Stubenhofer, A. Y. Timoshkin and M. Scheer, *Angew. Chem., Int. Ed.*, 2016, **55**, 14037–14040; (*f*) T. W. Mackewitz, D. Ullrich, U. Bergsträßer, S. Leininger and M. Regitz, *Liebigs Ann. Chem.*, 1997, **1997**, 1827–1839; (*g*) J. C. Guillemin, J. L. Cabioch, X. Morise, J. M. Denis, S. Lacombe, D. Gonbeau, G. Pfister-Guillouzo, P. Guenot and P. Savignac, *Inorg. Chem.*, 1993, **32**, 5021–5028.

12 Y. Wang, Y. Xie, P. Wei, R. B. King, H. F. Schaefer III, P. v. R. Schleyer and G. H. Robinson, *J. Am. Chem. Soc.*, 2008, **130**, 14970–14971.

13 O. Back, G. Kuchenbeiser, B. Donnadieu and G. Bertrand, *Angew. Chem., Int. Ed.*, 2009, **48**, 5530–5533.

14 D. Rottschäfer, M. K. Sharma, B. Neumann, H.-G. Stammler, D. M. Andrada and R. S. Ghadwal, *Chem.–Eur. J.*, 2019, **25**, 8127–8134.

15 M. K. Sharma, D. Rottschäfer, S. Blomeyer, B. Neumann, H.-G. Stammler, M. van Gastel, A. Hinz and R. S. Ghadwal, *Chem. Commun.*, 2019, **55**, 10408–10411.

16 (*a*) D. Rottschäfer, B. Neumann, H.-G. Stammler, R. Kishi, M. Nakano and R. S. Ghadwal, *Chem.–Eur. J.*, 2019, **25**, 3244–3247; (*b*) M. K. Sharma, S. Blomeyer, B. Neumann, H. G. Stammler and R. S. Ghadwal, *Chem.–Eur. J.*, 2019, **25**, 8249–8253; (*c*) M. K. Sharma, S. Blomeyer, B. Neumann, H.-G. Stammler, M. van Gastel, A. Hinz and R. S. Ghadwal, *Angew. Chem., Int. Ed.*, 2019, **58**, 17599–17603.

17 V. Lavallo, Y. Canac, C. Präsang, B. Donnadieu and G. Bertrand, *Angew. Chem., Int. Ed.*, 2005, **44**, 5705–5709.

18 No reaction between {(IPr)C(Ph)PCl_2} (**1**) and a weak π-acceptor NHC (IPr or SIPr) was observed under similar experimental conditions.

19 B. Manz, U. Bergsträßer, J. Kerth and G. Maas, *Chem. Ber.*, 1997, **130**, 779–788.

20 (*a*) O. Kühl, *Phosphorus-31 NMR Spectroscopy*, Springer-Verlag, Berlin Heidelberg, 2008; (*b*) V. B. Gudimetla, L. Ma, M. P. Washington, J. L. Payton, M. Cather Simpson and J. D. Protasiewicz, *Eur. J. Inorg. Chem.*, 2010, 854–865.

21 P. Pyykkö and M. Atsumi, *Chem.–Eur. J.*, 2009, **15**, 186–197.

22 F. Mathey, *Angew. Chem., Int. Ed.*, 2003, **42**, 1578–1604.

23 S. L. Hinchley, C. A. Morrison, D. W. H. Rankin, C. L. B. Macdonald, R. J. Wiacek, A. Voigt, A. H. Cowley, M. F. Lappert, G. Gundersen, J. A. C. Clyburne and P. P. Power, *J. Am. Chem. Soc.*, 2001, **123**, 9045–9053.